

Supporting Information

Platinated Porphyrin as a New Organelle and Nucleus Dual-targeted Photosensitizer for Photodynamic Therapy

Sizhe Zhu ^a, Si Yao ^a, Fengshou Wu ^{a*}, Lijun Jiang ^b, Ka-Leung Wong ^{b*}, Ji Zhou ^c, Kai Wang ^{a,c*}

^a Key Laboratory for Green Chemical Process of Ministry of Education, Wuhan Institute of Technology, Wuhan, P. R. China.

^b Department of Chemistry, Hong Kong Baptist University, Kowloon Tong, Hong Kong, P. R. China.

^c Hubei Key Lab of Novel Reactor & Green Chemical Technology, Wuhan Institute of Technology, Wuhan, P. R. China.

1. DNA binding affinity and mode

The binding constants (K) of Pt-Por-RB and Me-Por-RB were calculated by the equation (1).

$$[DNA]/\Delta\varepsilon_{ap}=[DNA]/\Delta\varepsilon+1/(\Delta\varepsilon K) \quad (1)$$

$$\Delta\varepsilon_{ap}=|\varepsilon_A-\varepsilon_F|; \quad \Delta\varepsilon=|\varepsilon_B-\varepsilon_F|;$$

Where the [DNA] is the CT DNA concentration, ε_A , ε_B , ε_F is the apparent extinction coefficient, the extinction coefficient of bound porphyrin and the extinction coefficient of free porphyrin. The fitting curves were shown in Fig S1.

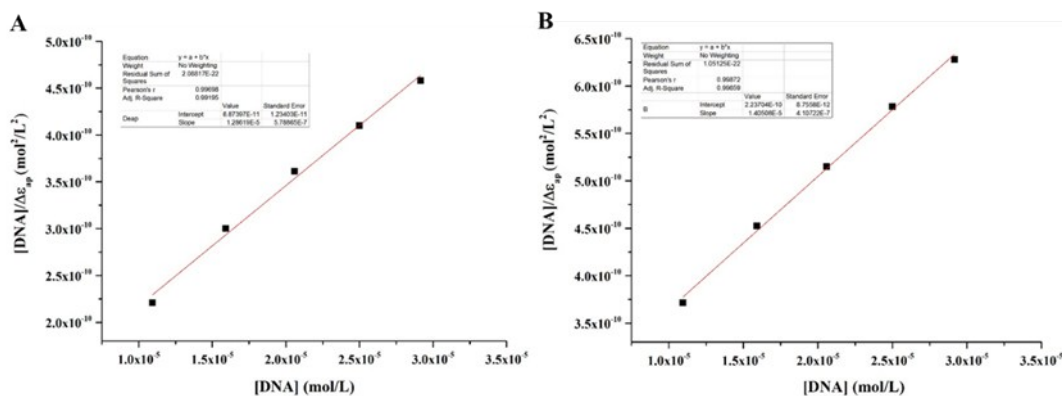


Fig. S1. The relations between the $[DNA]/\Delta \epsilon_{sp}$ and $[DNA]$ of (A) Pt-Por-RB; (B) Me-Por-RB

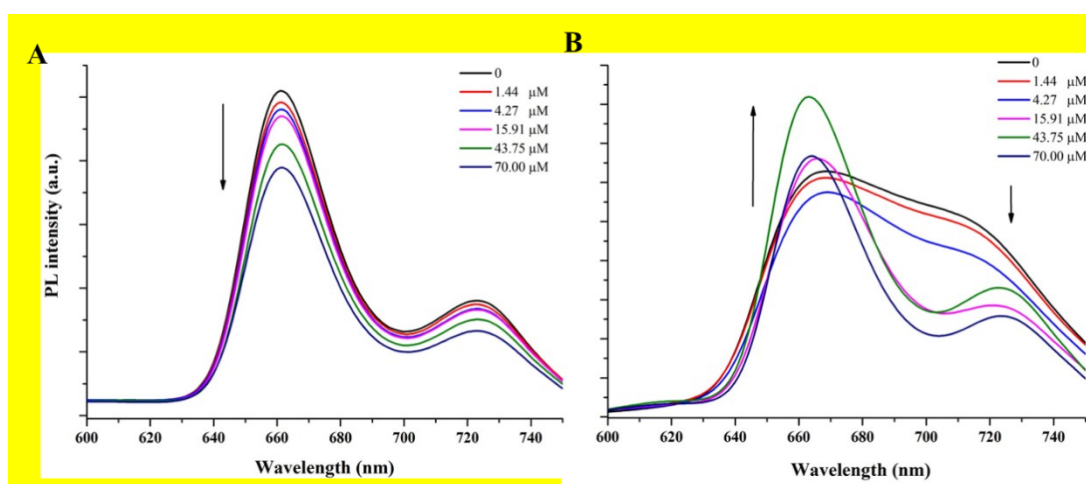


Fig. S2. Emission spectra of (A) Pt-Por-RB; (B) Me-Por-RB; with titration of CT DNA (from 0 to 70 μM)

The fluorescence spectrophotometric titrations of porphyrins with CT DNA (from 0 to 70 μM) were performed as shown in Fig. S2. The change of PL spectrum for Pt-Por-RB and Me-Por-RB were different after the addition of CT DNA. At low concentration of CT DNA (0 to 4.27 μM), the PL intensity of Me-Por-RB was only slightly reduced related to Pt-Por-RB (significantly decrease), probably due to the self-stacking of porphyrin on the surface of CT DNA. However, the emission spectrum of Me-Por-RB increased significantly when the concentration of DNA is beyond 4.27 μM , indicating the interaction mode between porphyrin and CT DNA was changed from self-stacking to intercalation at high concentration of CT DNA.

2. NMR and MS spectra of compounds

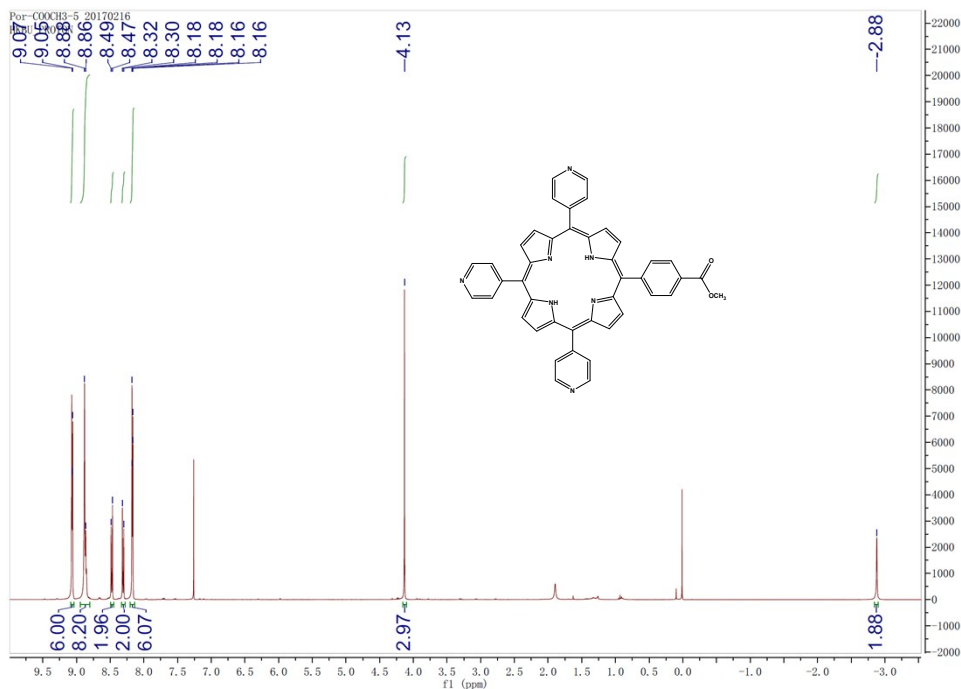


Fig. S3. $^1\text{H-NMR}$ (CDCl_3) spectrum of meso-5-(4'-carboxymethylphenyl)-10,15,20-tris(4'-pyridyl)porphyrin

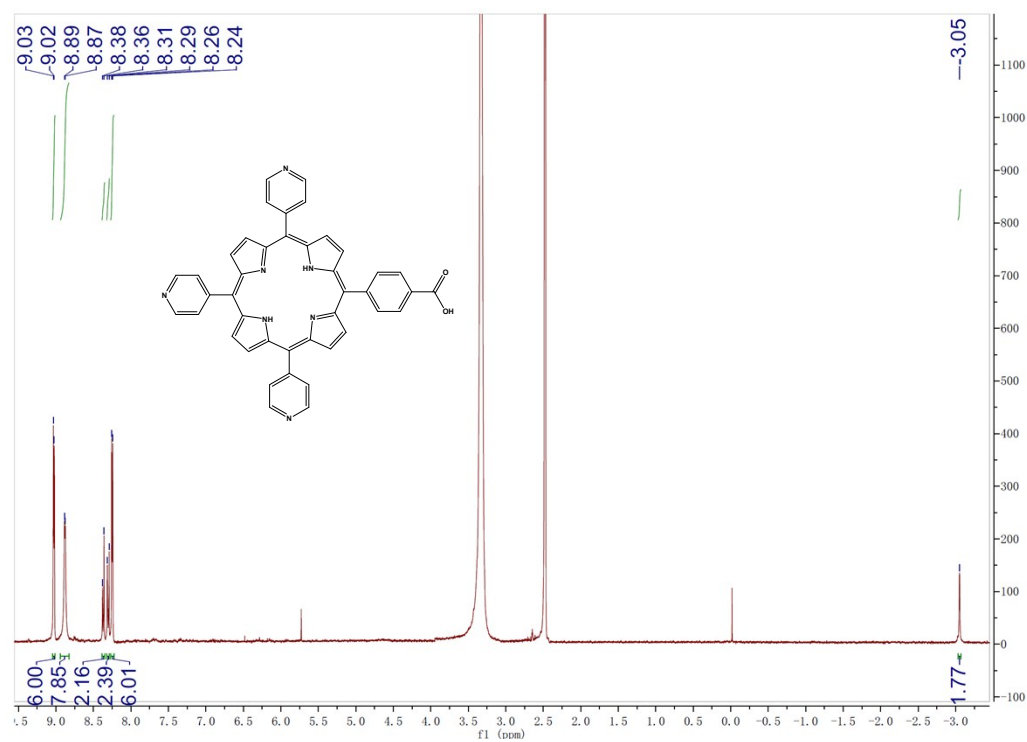


Fig. S4. $^1\text{H-NMR}$ (DMSO-d_6) spectrum of Por

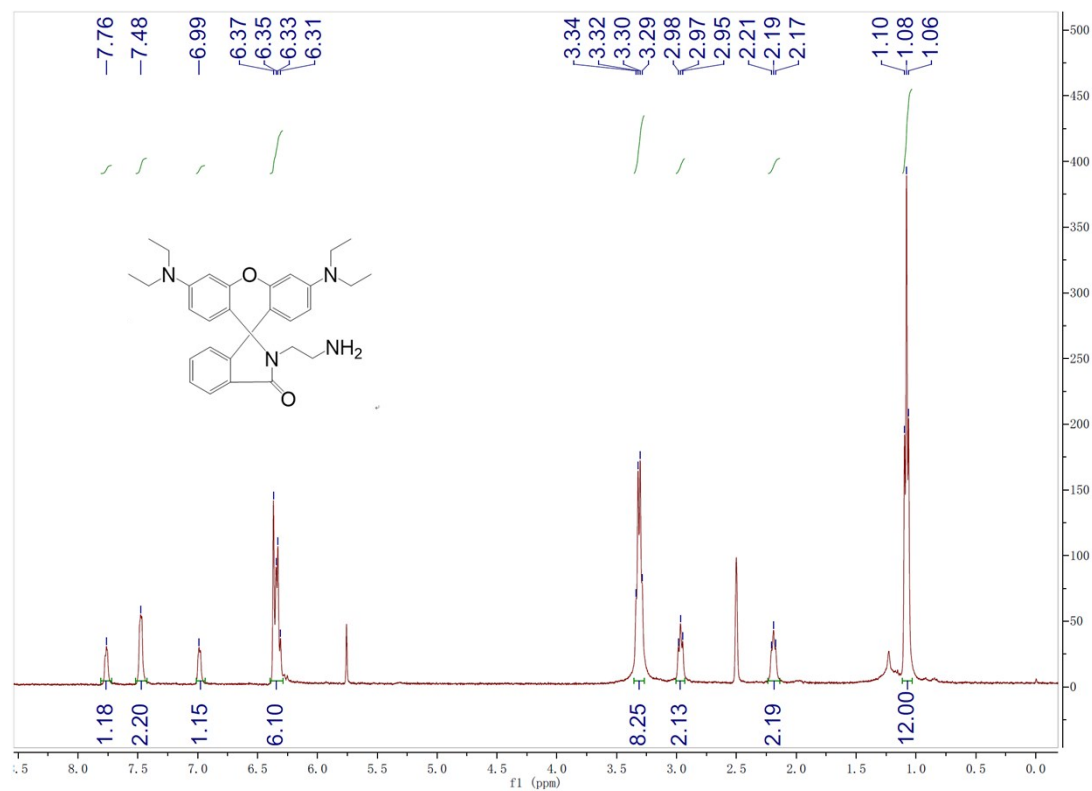


Fig. S5. $^1\text{H-NMR}$ (DMSO-d_6) spectrum of RB-NH $_2$

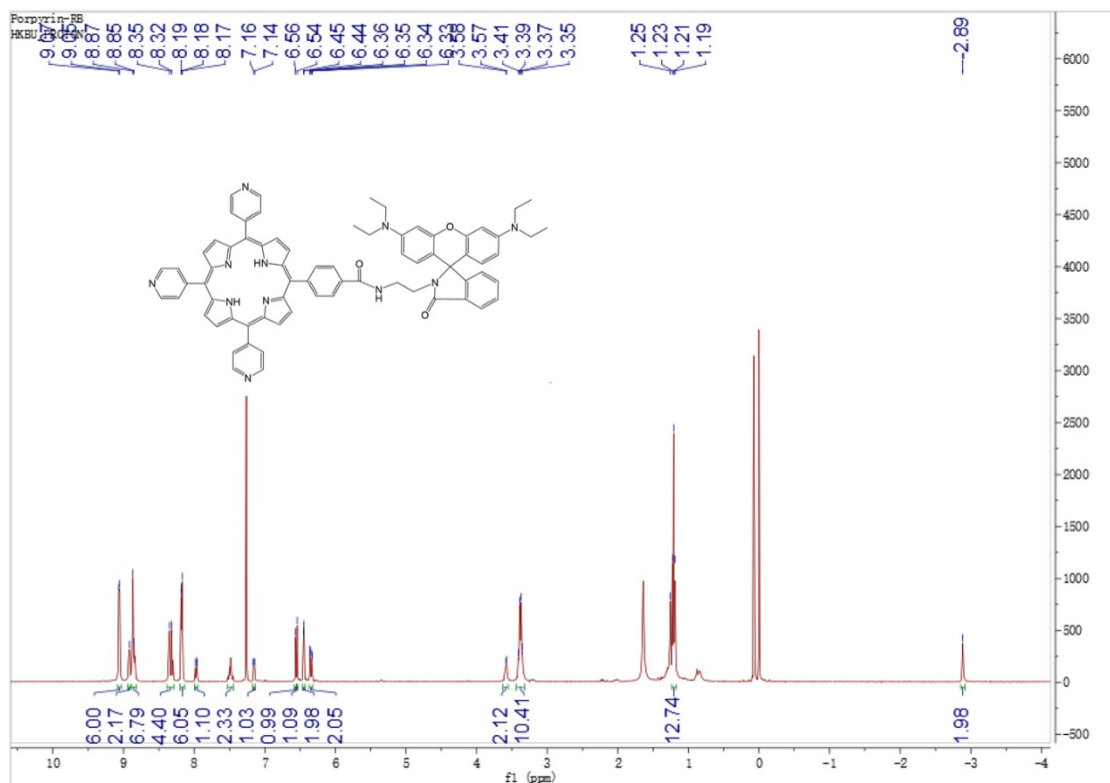


Fig. S6. $^1\text{H-NMR}$ (CDCl_3) spectrum of Por-RB

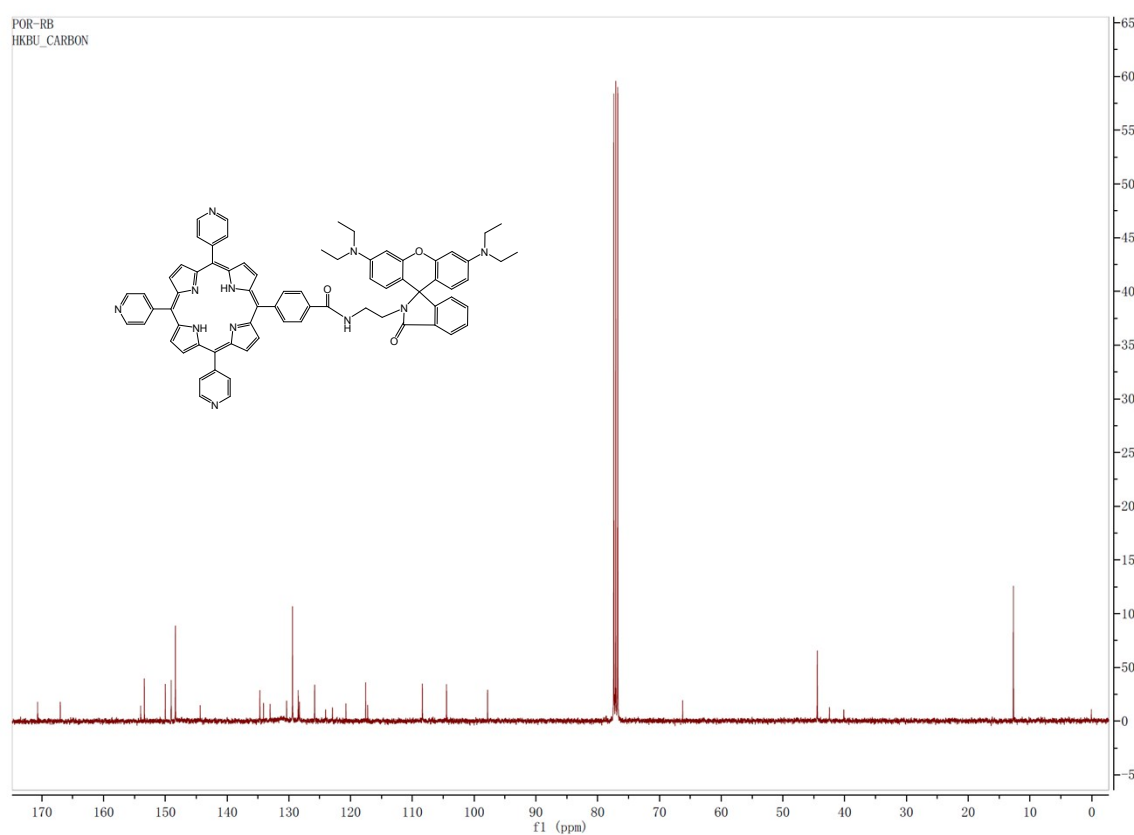


Fig.S7. $^{13}\text{C-NMR}$ (CDCl_3) spectrum of Por-RB

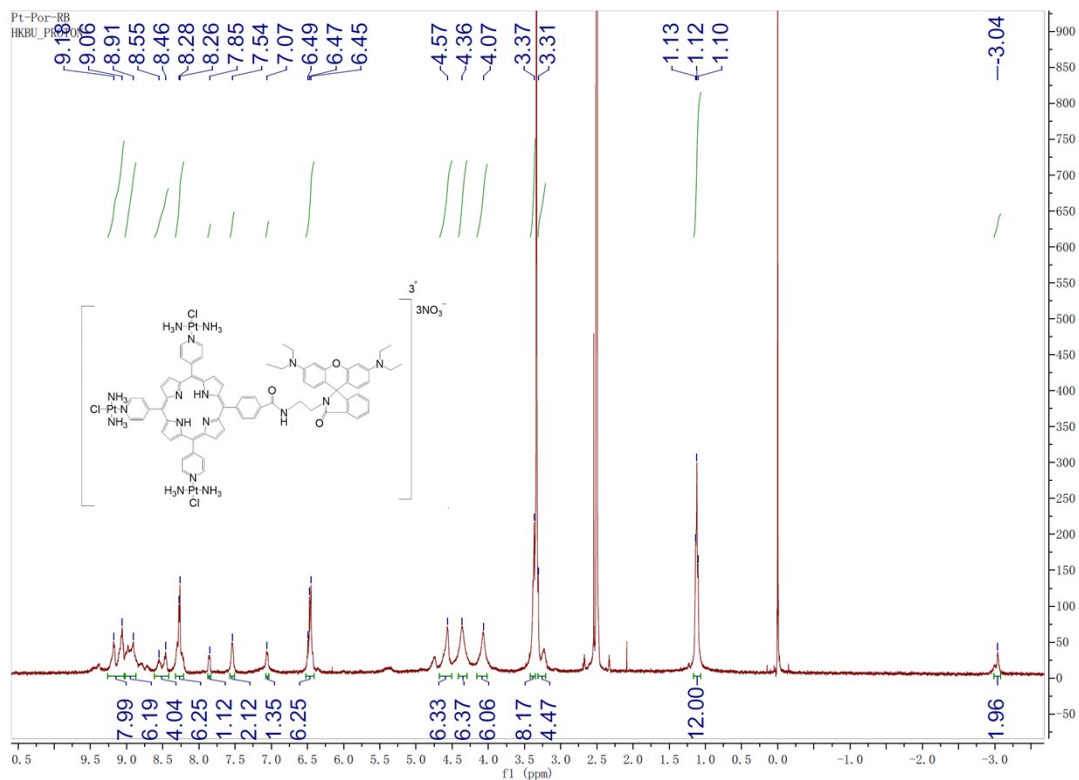


Fig. S8. ¹H-NMR (DMSO-d₆) spectrum of Pt-Por-RB

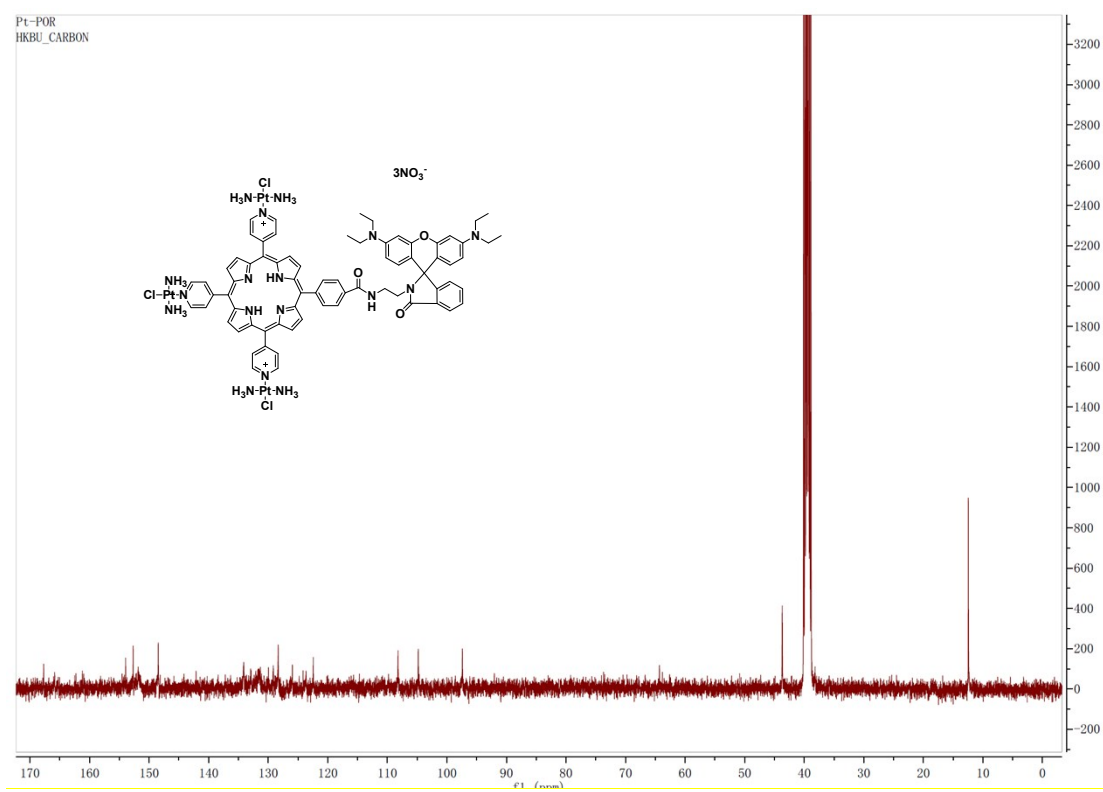


Fig.S9. ¹³C-NMR (DMSO-d₆) spectrum of Pt-Por-RB

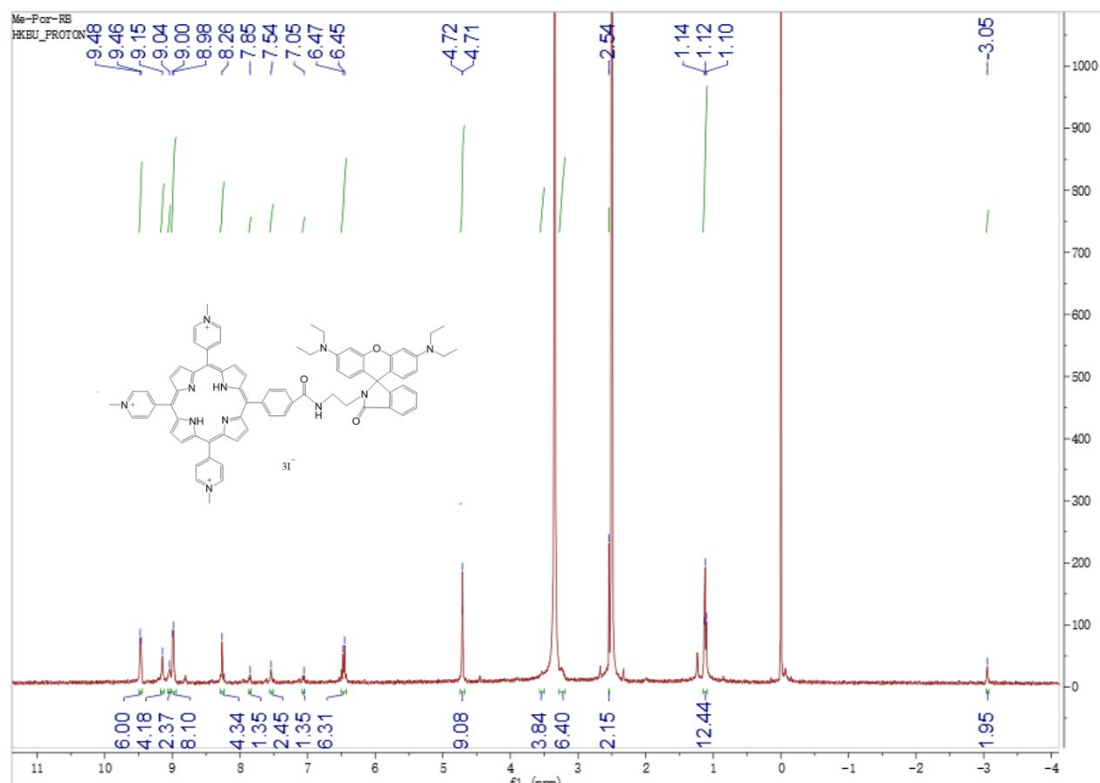


Fig. S10. $^1\text{H-NMR}$ (DMSO-d_6) spectrum of Me-Por-RB

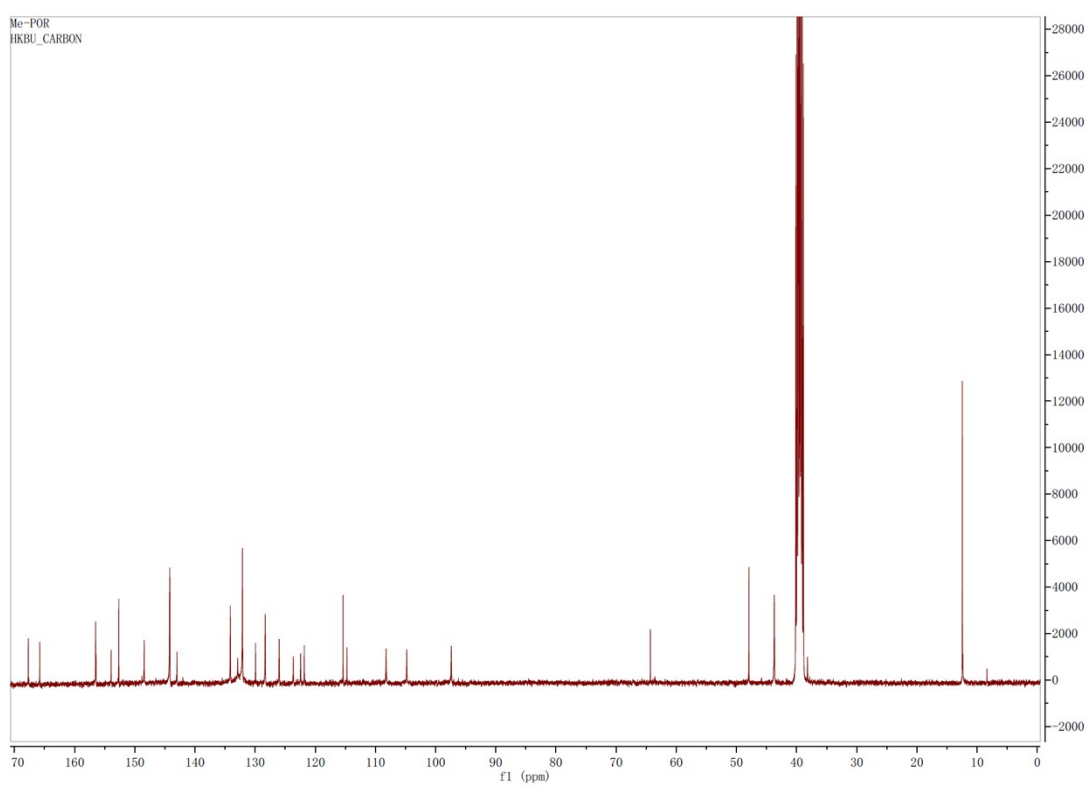


Fig.S11. $^{13}\text{C-NMR}$ (DMSO-d_6) spectrum of Me-Por-RB

HONG KONG BAPTIST UNIVERSITY, DEPARTMENT OF CHEMISTRY (MALDI-TOF)

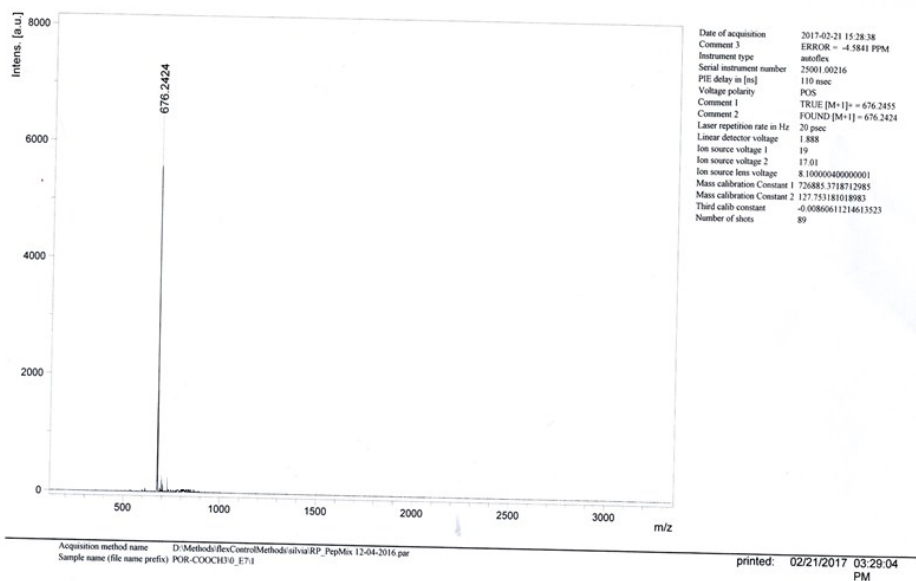


Fig. S12. MALDI-TOF spectrum of meso-5-(4'-carboxymethylphenyl)-10,15,20-tris(4'-pyridyl)porphyrin

HONG KONG BAPTIST UNIVERSITY, DEPARTMENT OF CHEMISTRY (MALDI-TOF)

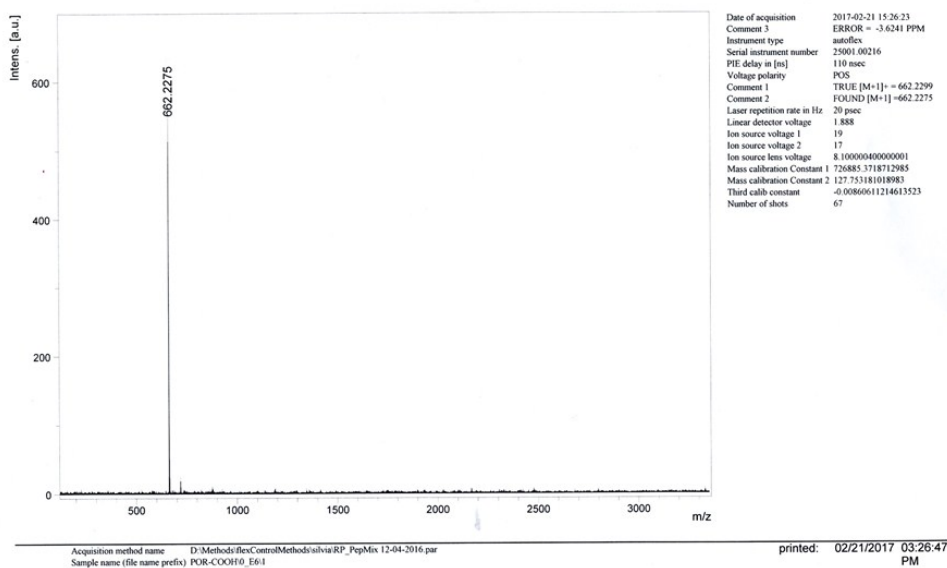


Fig. S13. MALDI-TOF spectrum of Por

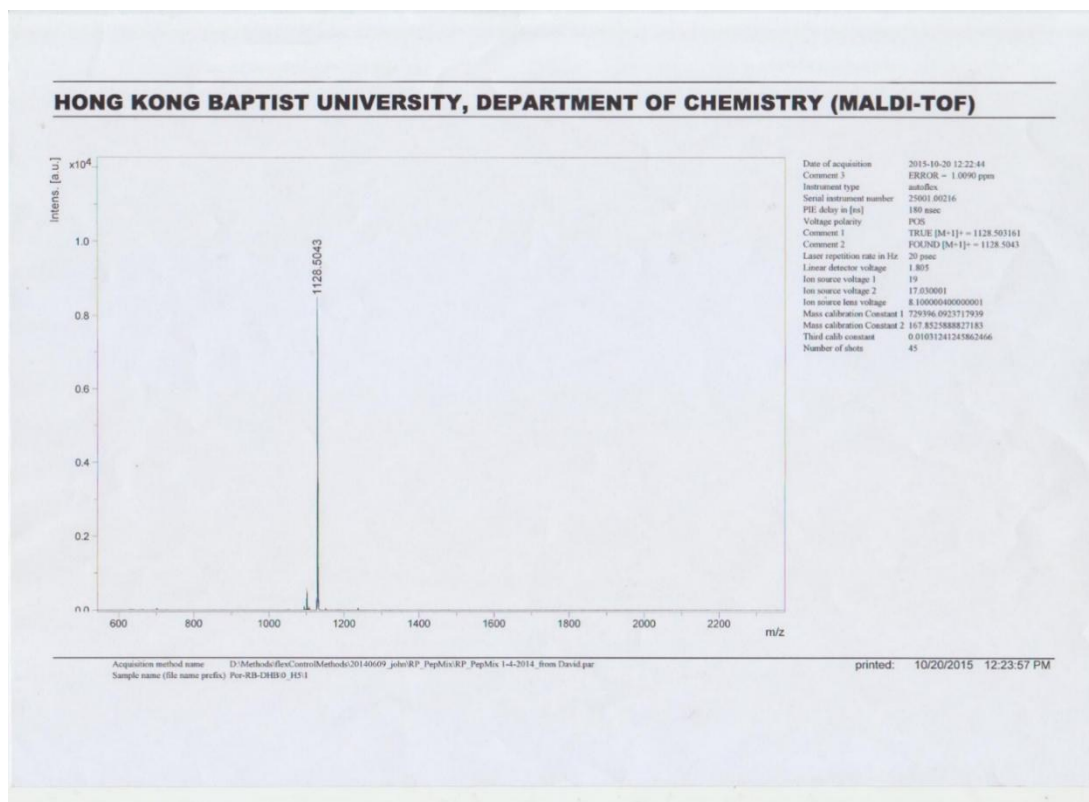


Fig. S14. MALDI-TOF spectrum of Por-RB

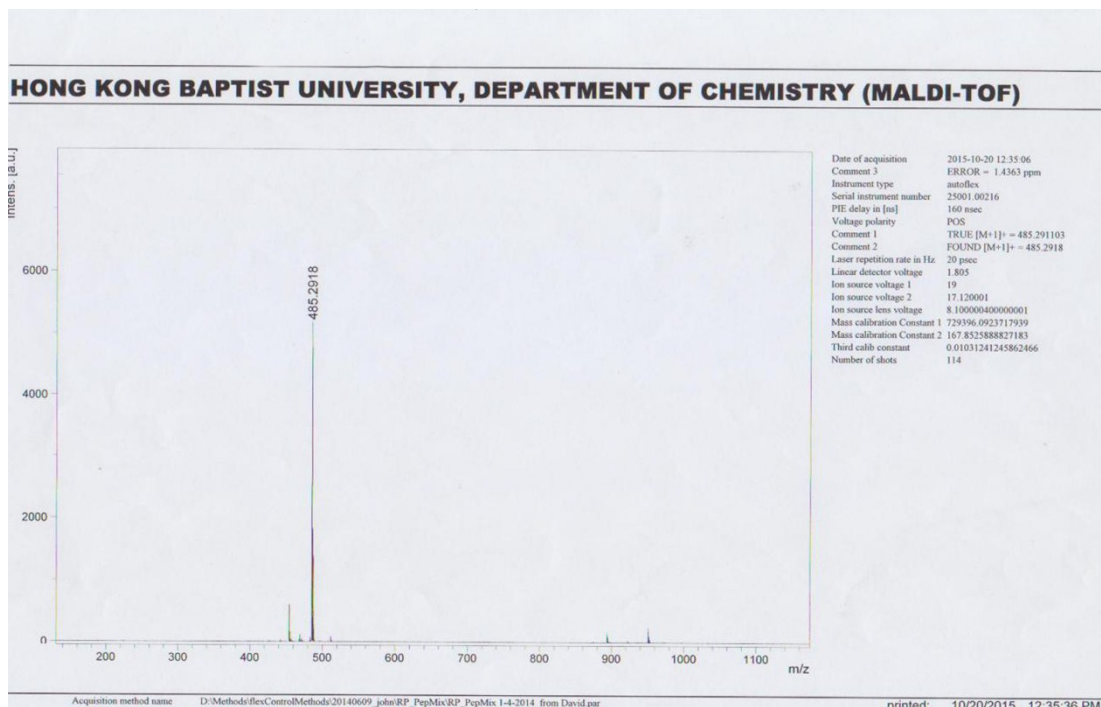


Fig.S15. MALDI-TOF spectrum of RhB-NH₂

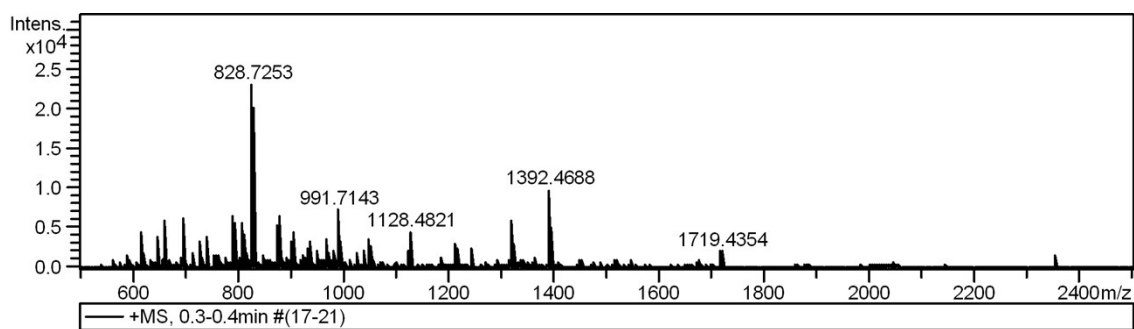


Fig. S16. ESI-MS spectrum of Pt-Por-RB

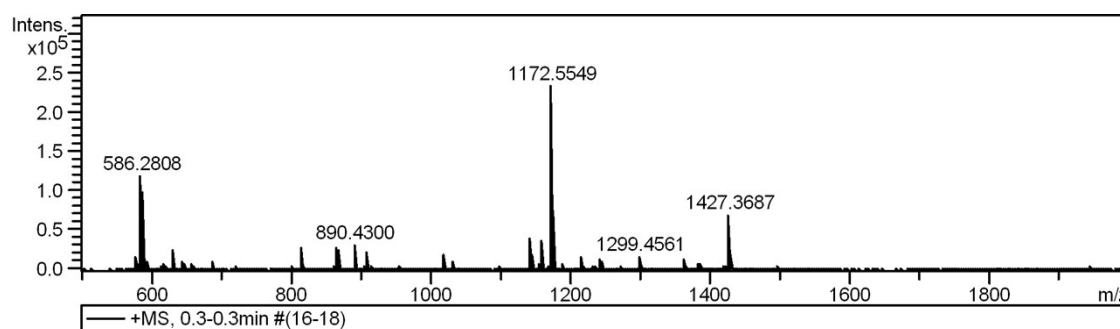


Fig. S17. ESI-MS spectrum of Me-Por-RB